Genes to Cells

BRIEF REPORT

R26-WntVis reporter mice showing graded response to Wnt signal levels

Tatsuya Takemoto[1,2]*, Takaya Abe[3], Hiroshi Kiyonari[3,4], Kazuki Nakao[4,5], Yasuhide Furuta[3,4], Hitomi Suzuki[1], Shinji Takada[6], Toshihiko Fujimori[3,7] and Hisato Kondoh[2,8]*

[1]*Fujii Memorial Institute of Medical Sciences, Tokushima University, 3-18-15 Kuramoto-cho, Tokushima 770-8503, Japan*
[2]*Graduate School of Frontier Biosciences, Osaka University, 1-3 Yamadaoka, Suita, Osaka 565-0871, Japan*
[3]*Genetic Engineering Team, RIKEN Center for Life Science Technologies, 2-2-3 Minatojima Minami-machi, Chuou-ku, Kobe 650-0047, Japan*
[4]*Animal Resource Development Unit, RIKEN Center for Life Science Technologies, 2-2-3 Minatojima Minami-machi, Chuou-ku, Kobe 650-0047, Japan*
[5]*Laboratory of Animal Resources, Center for Disease Biology and Integrative Medicine, Graduate School of Medicine, The University of Tokyo, Tokyo 113-0033, Japan*
[6]*Okazaki Institute for Integrative Bioscience, National Institutes of Natural Sciences, Okazaki, Aichi 444-8787, Japan*
[7]*Division of Embryology, National Institute for Basic Biology (NIBB), Okazaki, Aichi 444-8787, Japan*
[8]*Faculty of Life Sciences, Kyoto Sangyo University, Motoyama, Kamigamo, Kita-ku, Kyoto 603-8555, Japan*

The canonical Wnt signaling pathway plays a major role in the regulation of embryogenesis and organogenesis, where signal strength-dependent cellular responses are of particular importance. To assess Wnt signal levels in individual cells, and to circumvent the integration site-dependent bias shown in previous Wnt reporter lines, we constructed a new Wnt signal reporter mouse line R26-WntVis. Heptameric TCF/LEF1 binding sequences were combined with a viral minimal promoter to confer a graded response to the reporter depending on Wnt signal strengths. The histone H2B-EGFP fusion protein was chosen as the fluorescent reporter to facilitate single-cell resolution analyses. This WntVis reporter gene was then inserted into the *ROSA26* locus in an orientation opposite to that of the endogenous gene. The R26-WntVis allele was introduced into *Wnt3a*$^{-/-}$ and *Wnt3a*$^{vt/-}$ mutant mouse embryos and compared with wild-type embryos to assess its performance. The R26-WntVis reporter was activated in known Wnt-dependent tissues and responded in a graded fashion to signal intensity. This analysis also indicated that the major Wnt activity early in embryogenesis switched from Wnt3 to Wnt3a around E7.5. The R26-WntVis mouse line will be widely useful for the study of Wnt signal-dependent processes.

Introduction

Wnt signaling via the canonical intracellular pathway plays a central role in embryogenesis and organogenesis, providing tissue specificities and identities (review, Lien & Fuchs 2014). Growing evidence indicates that canonical Wnt signaling affects cells differently depending on the signal strength in individual cells (Lien & Fuchs 2014). Therefore, elucidation of Wnt signal-dependent events would be facilitated by the availability of Wnt reporter transgenic lines that allow for the assessment of Wnt signal strength with single-cell resolution.

Various Wnt reporter transgenic lines have been produced (Korinek *et al.* 1997; DasGupta & Fuchs 1999; Lustig *et al.* 2002; Maretto *et al.* 2003; Mohamed *et al.* 2004; Moriyama *et al.* 2007), but none has satisfied all

Communicated by: Tetsuya Taga
**Correspondence:* takemoto.tatsuya@tokushima-u.ac.jp or kondohh@cc.kyoto-su.ac.jp

DOI: 10.1111/gtc.12364

desired features. A common approach was to join multimeric TCF/LEF1 binding sites, acting as a Wnt-dependent enhancer, to a nonspecific promoter to activate the transcription of an enzyme or fluorescent protein gene, and such constructs were inserted in the mouse genome via random integration. These earlier Wnt-responsive transgenes displayed background (Wnt-independent) expression and tissue bias in Wnt-dependent gene activation, probably reflecting the local chromosomal environments (Al Alam *et al.* 2011).

Fusion proteins comprising histone H2B and fluorescent protein that accumulates in nuclei can offer an excellent reporter system to assess responses of individual responding cells (Kanda *et al.* 1998; Kurotaki *et al.* 2007; Abe *et al.* 2011). Ferrer-Vaquer *et al.* (2010) reported a Wnt reporter transgenic line, in which EGFP was fused to H2B, significantly improving the resolution. However, this line was also constructed using random transgene insertion. Moreover, the *hsp68* promoter used in the transgene provides minimally graded responses.

We first constructed a Wnt reporter transgene by combining the TCF/LEF1 sites, viral minimal promoter and sequence encoding the histone H2B-EGFP fusion protein. The transgene was then inserted into the *ROSA26* locus, which supports the most tissue-unbiased expression of exogenous genes (Zambrowicz *et al.* 1997; Soriano 1999). The transgene responded in a graded fashion to the Wnt signal levels in individual cells, as showed using hypomorphic *Wnt3a*$^{vt/-}$ heterozygote. This reporter transgene, designated as R26-WntVis (ROSA26-based Wnt signal visualizing reporter), will be useful for studies on Wnt-dependent developmental and organogenic processes.

Results and discussion

Rationale for the Wnt reporter design

It is widely appreciated that a nearly ubiquitous gene expression is attained by insertion of a protein-encoding sequence in the *ROSA26* gene locus. This feature of the *ROSA26* locus is conferred by the unique transcriptional competency of the chromosomal locus (Nyabi *et al.* 2009). Although the locus is transcribed from a nonspecific promoter (Kisseberth *et al.* 1999), previous reports indicate that exogenous genes in the *ROSA26* locus are more actively transcribed when inserted in the opposite rather than the same orientation as the endogenous transcripts (Strathdee *et al.* 2006; Nyabi *et al.* 2009). We sought to use the *ROSA26* locus to achieve tissue-unbiased and Wnt signal-dependent activation of the transgene.

An important decision in designing a reporter gene is whether to use a promoter with graded or with nongraded responses in combination with the multimeric TCF/LEF1 binding sites. A typical nongraded response promoter is the *hsp68* promoter, which was used in combination with various enhancers to produce transgenic mouse lines with highly tissue-specific expression (Rossant *et al.* 1991; Sasaki & Hogan 1996). However, to achieve graded outputs of Wnt signaling, we needed a promoter that would show a graded response to enhancers of various strengths. One such example is the HSVtk promoter, which we used in this study (Uchikawa *et al.* 2003; Takemoto *et al.* 2006). The transcripts starting from the promoter should encode a reporter protein to be detected with high sensitivity, such as fusion

Figure 1 Organization of the R26-WntVis reporter transgene and its expression in mouse embryos from E6.5 to E12. (A) Schematic representation of the WntVis transgene organization before integration into the mouse genome. 7 × TCF/LEF1, heptameric TCF/LEF1 binding sequences; tkPro, minimal promoter of the Herpes simplex virus thymidine kinase gene; H2B-EGFP-pA, transcriptional unit of the reporter gene, consisting of the coding sequence for the histone H2B-EGFP fusion protein and an SV40 late polyA addition signal; inverted 2 × pA, two copies of rabbit β-globin polyA signal placed to block transcription from downstream; arrow with lettering, direction of the endogenous transcription from *ROSA26* locus. The scheme is not drawn on scale. (B–G) R26-WntVis reporter activity at various developmental stages of mouse embryos. (B) EGFP fluorescence (right) in E6.5 embryo and differential interference contrast (DIC) image of the same embryo (left). The bar indicates 50 μm. (C) Stacked EGFP fluorescence images using a confocal microscope of an E7.5 embryo (right) and DIC image of the same embryo (left), showing the graded signal intensities toward the posterior side of the embryo. The bar indicates 200 μm. (D) An E8.5 embryo in lateral (left) and dorsal view (right), where bright-field and fluorescent images are compared. A strong signal was observed confined to the posterior tissues surrounding the primitive streak. The bars indicate 1 mm. (E) An E9.5 embryo, where new signal-positive tissues not observed at E8.5 have emerged, e.g., the dorsal midline of the brain, dorsal part of the otic placode and somites. The bar indicates 500 μm. (F) An E10.5 embryo, where the fluorescent signal was prominent in the otic placode, tip of the limb buds, and chordoneural hinge of the tail, confirmed using dissected portions of embryos. The bars indicate 500 μm. (G) An E12 embryo, where the signal in the roof of the forebrain, whisker placodes, mammary glands and apical ectodermal ridge (AER) are clearly visible by external inspection. The bar indicates 1 mm. Abbreviations: A, anterior; P, posterior; cnh, chordoneural hinge; ep, epiblast; fl, forelimb; hl, hindlimb; ie., inner ear; mg, mammary gland; op, otic placode; ps, primitive streak; rb, roof of brain; rf, roof of forebrain; sm, somites; tb, tail bud; wp, whisker placodes.

protein consisting of a fluorescent protein and a histone subunit that will be concentrated in a nucleus (Kanda *et al.* 1998; Kurotaki *et al.* 2007; Ferrer-Vaquer *et al.* 2010; Abe *et al.* 2011; Shioi *et al.* 2011).

We thus used the following protocol to construct and insert a Wnt reporter gene into the *ROSA26* locus. A heptameric TCF/LEF1 binding sequence was inserted upstream of herpes simplex virus thymidine kinase (HSVtk) promoter (220 bp) (Uchikawa *et al.* 2003) that controls the H2B-EGFP fusion protein transcription. Transcription is terminated by the SV40 late polyA signal inserted downstream of the coding sequence. Tandem polyA signals derived from

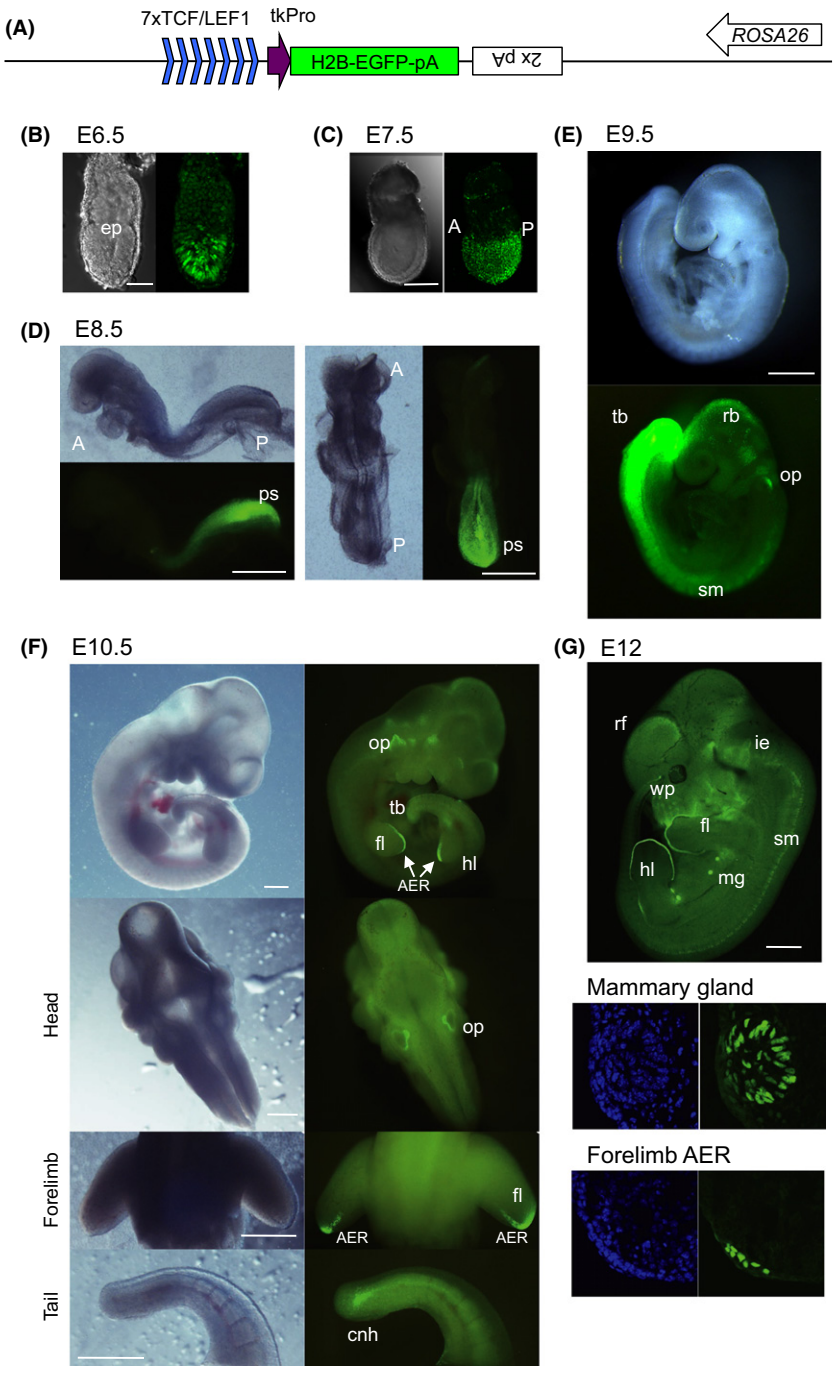

the rabbit β-globin gene were further inserted downstream of the gene in the opposite orientation to inhibit transcriptional read-through from the endogenous *ROSA26* promoter (Fig. 1A).

The transgene was inserted into the Gateway cassette (Hohenstein *et al.* 2008; Abe *et al.* 2011) to construct the gene-targeting vector for *ROSA26* locus integration with the transgene oriented opposite to that of the endogenous gene. Using this targeting vector, homologous recombinant ES cells were selected by neo-resistance. Wnt reporter mice were generated by injection of the ES cells carrying R26-WntVis into 8-cell stage embryos, and the *Neo* cassette was removed by crossing with the FLP recombinase-expressing mouse (Abe *et al.* 2011).

Wnt reporter activity in embryos at early stages of development

We investigated the Wnt reporter activity of R26-WntVis in mouse embryos during stages E6.5–E12. During these stages, Wnt3 and Wnt3a are the major Wnt proteins expressed and involved in the canonical pathway. Wnt3 expression begins in the epiblast before gastrulation, and its expression increases on the posterior side of embryos where gastrulation initiates (Liu *et al.* 1999). Wnt3 expression then becomes confined to the posterior epiblast and its adjacent visceral endoderm. After the initiation of gastrulation, Wnt3a begins to be expressed in the posterior epiblast (Takada *et al.* 1994). At the early head-fold stage (E7.25), Wnt3a continues to be expressed in the primitive streak region, whereas Wnt3 expression ceases. In the early somite stage (E8.5), Wnt3a is strongly expressed in the region of epiblast abutting the primitive streak and very weakly in the nascent mesoderm (Takemoto *et al.* 2011).

Strong R26-WntVis activity was detected in the epiblast of pregastrulation embryos (Fig. 1B). After initiation of gastrulation, the reporter activity became high in the posterior epiblast and adjacent visceral endoderm as shown in an E7.5 embryo (Fig. 1C), consistent with the endogenous Wnt expression patterns described above.

At E8.5, the Wnt reporter activity became prominent in the primitive streak and surrounding tissues at the posterior end of embryos (Fig. 1D) that included the notochord and epiblast abutting the primitive streak, the latter serving as neuro-mesodermal bipotential precursor called axial stem cells (Kondoh & Takemoto 2012). At E9.5, strong Wnt reporter activity in the growing posterior end of the trunk continued (Fig. 1E). In addition, the reporter activity was clearly visible in the somites, limb buds, dorsal aspect of the otic vesicle and the dorsal midline of the brain. The emergence of Wnt activity in this region of the brain corresponds to the expression of Wnt1 and Wnt3a (Parr *et al.* 1993). At E10.5, the Wnt reporter activity in the posterior end of the trunk significantly decreased with strong activity remaining only in the chordoneural hinge region (Fig. 1F). Strong Wnt reporter activity was observed in the otic placodes and apical ectodermal ridge (AER) of the limb buds. At E12, strong Wnt reporter activity was additionally observed in the developing mammary glands and whisker hair placodes (Fig. 1G). Analysis of individual cells in histological sections of E12 embryos through the hindlimb AER and rudimentary mammary gland showed strict localization of cell populations with signal input, indicating that Wnt signaling is short-ranged in these tissues.

Comparison to previously published Wnt reporters

Wnt signal detection during stages E11–E12 is compared between R26-WntVis and representative Wnt signal reporters (DasGupta & Fuchs 1999; Lustig *et al.* 2002; Maretto *et al.* 2003; Ferrer-Vaquer *et al.* 2010) in Table S1 (Supporting Information). All major tissues showing Wnt signaling in whole-mount specimens via other reporters were also positive using the R26-WntVis reporter. Positive tissues included the roof of the telencephalon, whisker placodes, inner ear, somites, limb AER, rudimentary mammary glands and tail tip. The fluorescent signals from the R26-WntVis reporter had no background, showing no indication of Wnt-independent responses. These features were also observed for the TCF/Lef:H2B-GFP reporter (Ferrer-Vaquer *et al.* 2010). However, response to Wnt signal levels are significantly different between R26-WntVis and TCF/Lef:H2B-GFP reporters, as will be discussed below.

Wnt reporter activity in Wnt3a-null mutants during early gastrulation stages

To test the analytical power of the R26-WntVis reporter, we introduced the reporter into *Wnt3a* homozygous mutant ($Wnt3a^{-/-}$) embryos and analyzed the reporter signals in comparison with wild-type embryos.

At the early head-fold stage (Downs & Davies 1993), the R26-WntVis reporter signal was already down-regulated in $Wnt3a^{-/-}$ embryos. However, the

distribution of the reporter activity was similar to that of *Wnt3a*$^{+/+}$ embryos, with the activity detected in the epiblast and some visceral enododermal cells and stronger signals toward the posterior side of the embryos (Fig. 2A). At the late head-fold stage, the R26-WntVis reporter activity in *Wnt3a*$^{-/-}$ embryos was decreased further (Fig. 2B), indicating that the major Wnt activity switches from Wnt3 to Wnt3a during the head-fold stages. Indeed, at the 2- to 3-somite stage, the Wnt reporter activity was strong in tissues and areas surrounding the primitive streak in *Wnt3a*$^{+/+}$ embryos but negligible in *Wnt3a*$^{-/-}$ embryos (Fig. 2C).

These observations indicated that the H2B-EGFP fusion protein derived from the R26-WntVis transgene is lost from the nucleus fairly quickly after the Wnt signaling is turned off, although normal (untagged) histones are considered to be long-lived. Thus, the WntVis reporter is suitable not only for the analysis of spatial distribution of signal strength, but also for the analysis of temporal changes in Wnt signaling.

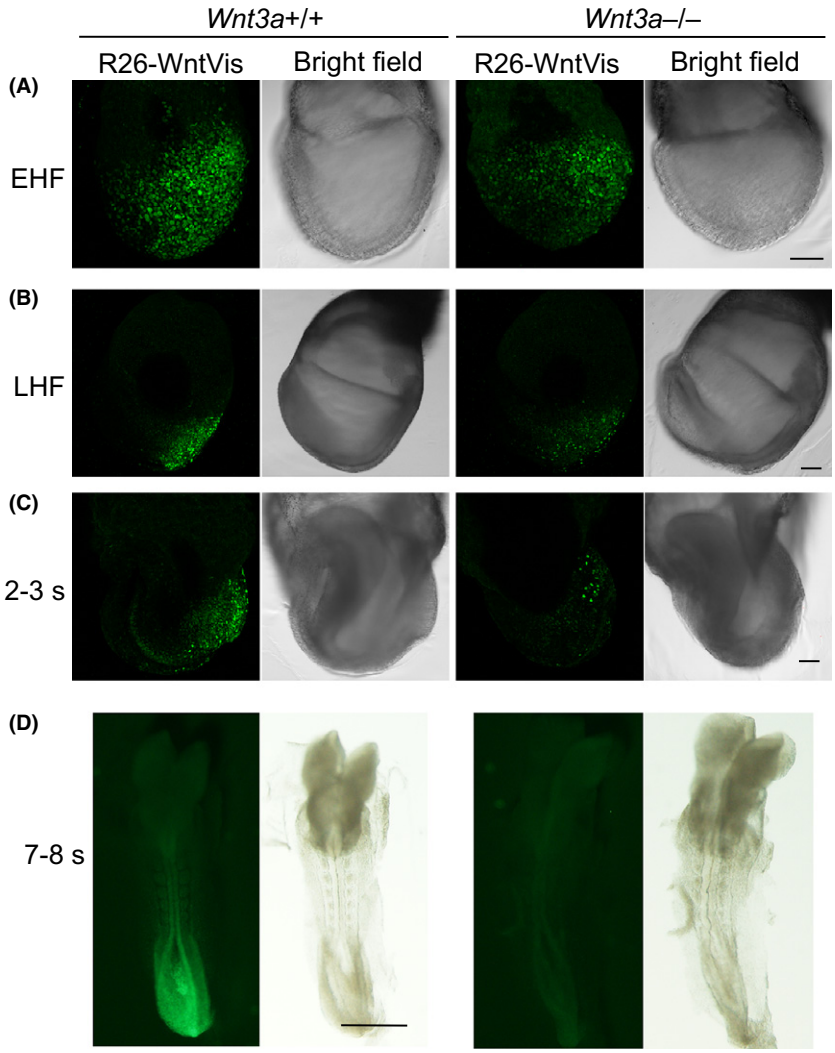

Figure 2 R26-WntVis reporter signals in *Wnt3a*$^{+/+}$ and *Wnt3a*$^{-/-}$ embryos. (A–C) Embryos at the early head-fold (EHF) (A), late head-fold (LHF) (B) and 2- to 3-somite (2–3 s) stages (C). Stacked EGFP fluorescence images using a confocal microscope of the embryos are presented in comparison with the bright-field images on the right. The bars indicate 100 μm. (D) E8.5 (7- to 8-somite stage) embryos showing fluorescent signal of R26-WntVis, which is grossly absent in *Wnt3a*$^{-/-}$ embryos (right). The bar indicates 200 μm.

Wnt3a$^{-/-}$ embryos fail to develop paraxial mesoderm approximately posterior to somite 8, because the maintenance of axial stem cells in the posterior trunk depends on Wnt signal input (Garriock *et al.* 2015) and the paraxial mesoderm precursors that have ingressed through the primitive streak develop as ectopic neural tissue (Takada *et al.* 1994; Yoshikawa *et al.* 1997). We investigated the distribution of cellular Wnt signal inputs at the 7- to 8-somite stage using R26-WntVis transgenic embryos (Fig. 2D). In the whole-mount view, *Wnt3a*$^{+/+}$ embryos displayed strong Wnt signaling in tissues proximal to the primitive streak (Fig. 2D). In contrast, *Wnt3a*$^{-/-}$ embryos overtly lacked these signals, including the primitive streak-proximal tissues (Fig. 2D), confirming that Wnt3a is the major Wnt ligand of canonical pathway during these stages.

Differential Wnt signal inputs at E8.5 (7- to 8-somite stage) comparing Wnt3a$^{+/+}$ and Wnt3a$^{vt/-}$ embryos

We investigated the responses of R26-WntVis transgene in embryos with altered Wnt signal levels. *Wnt3a*$^{+/-}$ heterozygous embryos were found to express a *Wnt3a* transcript level indistinguishable from *Wnt3a*$^{+/+}$ wild-type embryos, as assessed by *in situ* hybridization (data not shown), suggesting a regulatory feedback mechanism to sustain the *Wnt3a* expression level. However, the *Wnt3a* transcript level was reduced in *Wnt3a*$^{vt/-}$ heterozygous embryos with a hypomorphic *vestigial tail* (*vt*) allele (Greco *et al.* 1996) compared with sibling *Wnt3a*$^{+/+}$ embryos (Fig. 3A). The R26-WntVis signal in the region abutting the primitive streak was also reduced in *Wnt3a*$^{vt/-}$ embryos (Fig. 3B).

R26-WntVis signals in individual cells were examined using a series of cross-sections at axial levels posterior to the node (Fig. 3C). In *Wnt3a*$^{+/+}$ embryos, the epiblast abutting the primitive streak showed a stronger R26-WntVis signal in their nuclei than cells in the primitive streak or paraxial mesoderm. Similar tissue-dependent differences in R26-WntVis signals were also observed in *Wnt3a*$^{vt/-}$ embryos, although overall signal intensities were reduced as compared to *Wnt3a*$^{+/+}$ embryos.

To validate the differences in R26-WntVis responses among tissues and between genotypes, we measured relative fluorescence intensities of 40 randomly selected nuclei in each of the epiblast (E), primitive streak (P) and mesoderm (M) tissues (Fig. S2 in Supporting Information). The results shown in Fig. 3D indicate considerable variations in Wnt signal levels within a tissue, which was also evident by visual inspection, but the differences in average R26-WntVis signal levels between tissues was evident (Fig. 3E). Analysis of genotype dependence of R26-WntVis signal intensity in individual tissues indicated interesting differences. Although the R26-WntVis signal intensities in the epiblast and paraxial mesoderm were significantly reduced in *Wnt3a*$^{vt/-}$ embryos, they were not significantly affected in the primitive streak. This raises the interesting possibility that cells in the primitive streak regulate intracellular signaling to sustain a level, which compensates for the reduction in external Wnt signals.

Finally, we should mention the difference in the response to Wnt signal intensities between the R26-WntVis and the previously published TCF/Lef:H2B-GFP reporters (Ferrer-Vaquer *et al.* 2010), which have analogous TCF/Lef1 site multimers but bear different promoters, HSVtk for the graded response and *hsp68* for the less graded response, respectively. We examined an online version of a figure panel (Fig. 7A5) of Ferrer-Vaquer *et al.* (2010) as an example of the TCF/Lef:H2B-GFP response, in comparison with a stage- and position-matched node-level cross-section of an E8.5 R26-WntVis embryo, assuming published online data maintains the original linearity between fluorescence intensity and its photorecording. In these sections, the ventral node displayed a higher Wnt response than the epiblast and paraxial mesoderm. Relative signal intensities in the nuclei of these tissues were investigated (Fig. S3 in Supporting Information). The R26-WntVis reporter responded to Wnt signals with large tissue-dependent variations, whereas the TCF/Lef:H2B-GFP response was within a narrow range. It was also noted that TCF/Lef:H2B-GFP produces a high reporter signal with a low level of signal inputs indicated by R26-WntVis data. However, this occurs at the expense of a graded response to Wnt signal strengths. Which type of reporter suits will depend on the aim of investigation.

Experimental procedures

Production of the R26-WntVis reporter mouse line

Heptameric TCF/LEF1 binding sequence, human histone H2B cDNA sequence and reversely oriented two copies of the rabbit β-globin polyA addition sequence were inserted into the *Sma*I, *Age*I and *Sal*I sites, respectively, of ptkEGFP

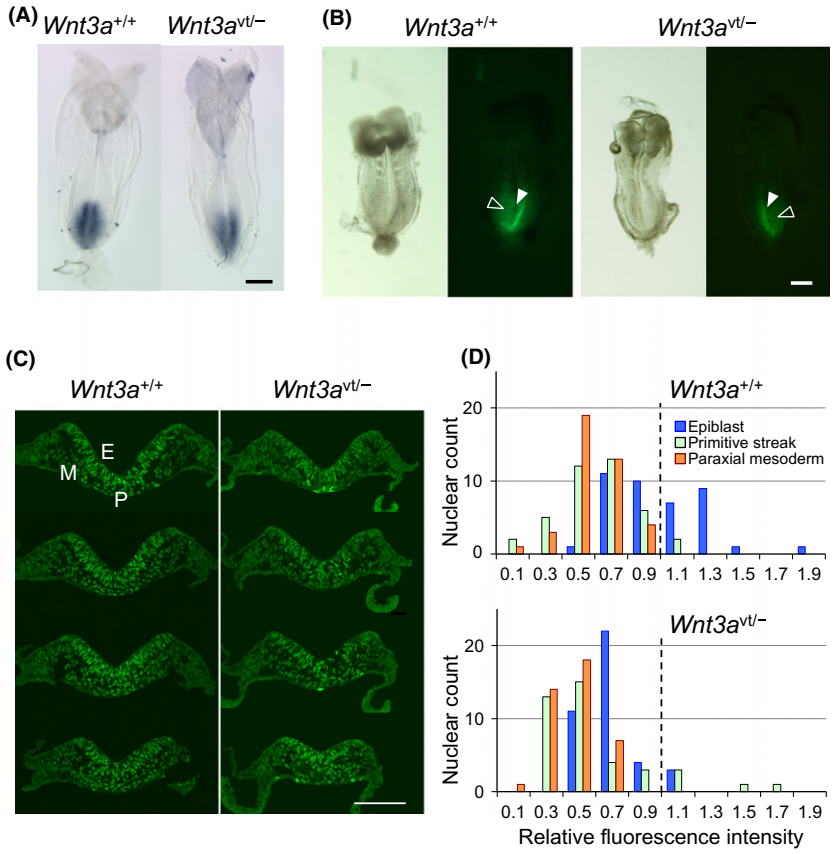

(E)

	Relative fluorescence intensity/nucleus			One-way ANOVA scores
	Epiblast	Primitive streak	Paraxial mesoderm	
Wnt3a$^{+/+}$	1.00 ± 0.30	0.60 ± 0.22	0.57 ± 0.17	F(2, 117) = 42 *P* = 0.0000001
t-test scores comparing the genotypes	*P* = 0.0016	*P* = 0.77	*P* = 0.0009	
Wnt3a$^{vt/-}$	0.69 ± 0.17	0.58 ± 0.34	0.45 ± 0.13	F(2, 117) = 10 *P* = 0.00007

Figure 3 Comparison of R26-WntVis signal between *Wnt3a*$^{+/+}$ and *Wnt3a*$^{vt/-}$ embryos. A. Comparison of *Wnt3a* in situ hybridization signals between sibling *Wnt3a*$^{+/+}$ and *Wnt3a*$^{vt/-}$ embryos at E8.5 showing reduced *Wnt3a* expression in the latter. The bar indicates 200 μm. B. Comparison of R26-WntVis signal between sibling *Wnt3a*$^{+/+}$ and *Wnt3a*$^{vt/-}$ embryos at E8.5. Bright-field images on the left and EGFP fluorescence on the right were compared. Solid white arrowheads indicate the node position, whereas open arrowheads indicate the epiblast area abutting the primitive streak where a decrease in the R26-WntVis signal in the *Wnt3a*$^{vt/-}$ embryo is appreciable. The bar indicates 200 μm. C. R26-WntVis signals in serial cryosections at levels posterior to the node of *Wnt3a*$^{+/+}$ and *Wnt3a*$^{vt/-}$ embryos shown in B. The bar indicates 100 μm. Regardless of the genotype, the signals observed in the epiblast (E) were generally higher than those in the primitive streak (PS) or paraxial mesoderm (M). Moreover, a general reduction in R26-WntVis fluorescence signals was noted for *Wnt3a*$^{vt/-}$ embryos. To quantitate the differences in the R26-WntVis signals, 40 nuclei were randomly chosen from these sections for each of the three tissues in each genotype, and fluorescence intensities in individual nuclei were quantified using Image J (Schneider *et al.* 2012). The actual nuclei chosen for the analysis are indicated in Fig. S2. D. Histograms of the distribution of fluorescence intensities derived from the analysis of the sections shown in C. The data are normalized to the mean of signals in the epiblast nuclei of *Wnt3a*$^{+/+}$ embryos, as indicated by broken vertical lines. It is evident that the fluorescence in the nuclei in the epiblast and paraxial mesoderm was reduced in *Wnt3a*$^{vt/-}$ embryos to approximately two-thirds of the level of *Wnt3a*$^{+/+}$ embryos. However, the fluorescence in the primitive streak was not significantly affected. E. Statistics that validate the above conclusions. Mean ± standard deviations, one-way ANOVA scores to compare tissues from individual genotypes, and two-tailed *t*-test scores comparing tissues between two genotypes are shown.

(Uchikawa *et al.* 2003) to produce pWntVis (Fig. S1 in Supporting Information). To generate target vector, the blunt-ended *Kpn*I and *Spe*I fragment of pWntVis was inserted into the *Xmn*I site of pENTR2B (pENTR2B-WntVis). Separately, *Neo* cassette (neomycin-resistant gene with *Pgk1* promoter and polyA signal sequence) flanked by FRT was inserted into pMC1-DT-A-ROSA26 (Abe *et al.* 2011), then the WntVis sequence was inserted using the Gateway system (Abe *et al.* 2011). This targeting vector was electroporated into HK3i ES cells (Kiyonari *et al.* 2010), and G418-resistant colonies were screened by PCR using primers 5′-TTGGGCTAGCACG CGTAAGAGCTCG-3′ (forward) and 5′-TTGACTCCTAG ACTTGTGACCCAGC-3′ (reverse) to detect homologous recombinants (3.4 kb), and the candidates were further tested by Southern hybridization. The homologous recombinant ES cells were injected into 8-cell stage ICR embryos to generate germ-line chimeras, which were then crossed with Tg (ACTFLPe)9205Dym/J mice to remove the *Neo* cassette, establishing the R26-WntVis reporter line. Embryos were genotyped using yolk sac DNAs by PCR using primers shown in Table S2 (Supporting Information). *Wnt3a*^{vt} allele was genotyped using unpublished primer information provided by Chikara Meno. All experiments using animals were carried out in Osaka University, Tokushima University, and RIKEN Center for Life Science Technologies, in accordance with guidelines of respective institutions.

Immunohistology and microscopy

Embryos were fixed for 5 h with 4% paraformaldehyde in PBS, passed through 15% and 25% sucrose in PBS, and embedded in OCT compound (Sakura Finetek), and made into cryosections with thickness of 7 μm. EGFP fluorescence images were taken using an M205FA microscope (Leica) with DP73 CCD camera (Olympus), or FV1200 confocal microscope (Olympus), and fluorescent intensities of individual nuclei were measured using Image J (Schneider *et al.* 2012).

Acknowledgements

We thank C. Meno of Kyusu University for provision of information concerning *vt* mutant allele genotyping. This study was supported by Grants-in-Aid for Scientific Research 24116707 and 24687029 to TT, and 22247035 and 26251024 to HK from MEXT Japan, Mitsubishi Foundation Grant to TT, and National Institute for Basic Biology Collaborative Research Grant.

References

Abe, T., Kiyonari, H., Shioi, G., Inoue, K., Nakao, K., Aizawa, S. & Fujimori, T. (2011) Establishment of conditional reporter mouse lines at ROSA26 locus for live cell imaging. *Genesis* **49**, 579–590.

Al Alam, D., Green, M., Tabatabai Irani, R., Parsa, S., Danopoulos, S., Sala, F.G., Branch, J., El Agha, E., Tiozzo, C., Voswinckel, R., Jesudason, E.C., Warburton, D. & Bellusci, S. (2011) Contrasting expression of canonical Wnt signaling reporters TOPGAL, BATGAL and Axin2(LacZ) during murine lung development and repair. *PLoS One* **6**, e23139.

DasGupta, R. & Fuchs, E. (1999) Multiple roles for activated LEF/TCF transcription complexes during hair follicle development and differentiation. *Development* **126**, 4557–4568.

Downs, K.M. & Davies, T. (1993) Staging of gastrulating mouse embryos by morphological landmarks in the dissecting microscope. *Development* **118**, 1255–1266.

Ferrer-Vaquer, A., Piliszek, A., Tian, G., Aho, R.J., Dufort, D. & Hadjantonakis, A.K. (2010) A sensitive and bright single-cell resolution live imaging reporter of Wnt/ss-catenin signaling in the mouse. *BMC Dev. Biol.* **10**, 121.

Garriock, R.J., Chalamalasetty, R.B., Kennedy, M.W., Canizales, L.C., Lewandoski, M. & Yamaguchi, T.P. (2015) Lineage tracing of neuromesodermal progenitors reveals novel Wnt-dependent roles in trunk progenitor cell maintenance and differentiation. *Development* **142**, 1628–1638.

Greco, T.L., Takada, S., Newhouse, M.M., McMahon, J.A., McMahon, A.P. & Camper, S.A. (1996) Analysis of the vestigial tail mutation demonstrates that Wnt-3a gene dosage regulates mouse axial development. *Genes Dev.* **10**, 313–324.

Hohenstein, P., Slight, J., Ozdemir, D.D., Burn, S.F., Berry, R. & Hastie, N.D. (2008) High-efficiency Rosa26 knock-in vector construction for Cre-regulated overexpression and RNAi. *Pathogenetics* **1**, 3.

Kanda, T., Sullivan, K.F. & Wahl, G.M. (1998) Histone-GFP fusion protein enables sensitive analysis of chromosome dynamics in living mammalian cells. *Curr. Biol.* **8**, 377–385.

Kisseberth, W.C., Brettingen, N.T., Lohse, J.K. & Sandgren, E.P. (1999) Ubiquitous expression of marker transgenes in mice and rats. *Dev. Biol.* **214**, 128–138.

Kiyonari, H., Kaneko, M., Abe, S. & Aizawa, S. (2010) Three inhibitors of FGF receptor, ERK, and GSK3 establishes germline-competent embryonic stem cells of C57BL/6N mouse strain with high efficiency and stability. *Genesis* **48**, 317–327.

Kondoh, H. & Takemoto, T. (2012) Axial stem cells deriving both posterior neural and mesodermal tissues during gastrulation. *Curr. Opin. Genet. Dev.* **22**, 374–380.

Korinek, V., Barker, N., Morin, P.J., van Wichen, D., de Weger, R., Kinzler, K.W., Vogelstein, B. & Clevers, H. (1997) Constitutive transcriptional activation by a beta-catenin-Tcf complex in APC-/- colon carcinoma. *Science* **275**, 1784–1787.

Kurotaki, Y., Hatta, K., Nakao, K., Nabeshima, Y. & Fujimori, T. (2007) Blastocyst axis is specified independently of early cell lineage but aligns with the ZP shape. *Science* **316**, 719–723.

Lien, W.H. & Fuchs, E. (2014) Wnt some lose some: transcriptional governance of stem cells by Wnt/beta-catenin signaling. *Genes Dev.* **28**, 1517–1532.

Liu, P., Wakamiya, M., Shea, M.J., Albrecht, U., Behringer, R.R. & Bradley, A. (1999) Requirement for Wnt3 in vertebrate axis formation. *Nat. Genet.* **22**, 361–365.

Lustig, B., Jerchow, B., Sachs, M., Weiler, S., Pietsch, T., Karsten, U., van de Wetering, M., Clevers, H., Schlag, P.M., Birchmeier, W. & Behrens, J. (2002) Negative feedback loop of Wnt signaling through upregulation of conductin/axin2 in colorectal and liver tumors. *Mol. Cell. Biol.* **22**, 1184–1193.

Maretto, S., Cordenonsi, M., Dupont, S., Braghetta, P., Broccoli, V., Hassan, A.B., Volpin, D., Bressan, G.M. & Piccolo, S. (2003) Mapping Wnt/beta-catenin signaling during mouse development and in colorectal tumors. *Proc. Natl Acad. Sci. USA* **100**, 3299–3304.

Mohamed, O.A., Clarke, H.J. & Dufort, D. (2004) Beta-catenin signaling marks the prospective site of primitive streak formation in the mouse embryo. *Dev. Dyn.* **231**, 416–424.

Moriyama, A., Kii, I., Sunabori, T., Kurihara, S., Takayama, I., Shimazaki, M., Tanabe, H., Oginuma, M., Fukayama, M., Matsuzaki, Y., Saga, Y. & Kudo, A. (2007) GFP transgenic mice reveal active canonical Wnt signal in neonatal brain and in adult liver and spleen. *Genesis* **45**, 90–100.

Nyabi, O., Naessens, M., Haigh, K., *et al.* (2009) Efficient mouse transgenesis using Gateway-compatible ROSA26 locus targeting vectors and F1 hybrid ES cells. *Nucleic Acids Res.* **37**, e55.

Parr, B.A., Shea, M.J., Vassileva, G. & McMahon, A.P. (1993) Mouse Wnt genes exhibit discrete domains of expression in the early embryonic CNS and limb buds. *Development* **119**, 247–261.

Rossant, J., Zirngibl, R., Cado, D., Shago, M. & Giguere, V. (1991) Expression of a retinoic acid response element-hsplacZ transgene defines specific domains of transcriptional activity during mouse embryogenesis. *Genes Dev.* **5**, 1333–1344.

Sasaki, H. & Hogan, B.L. (1996) Enhancer analysis of the mouse HNF-3 beta gene: regulatory elements for node/notochord and floor plate are independent and consist of multiple sub-elements. *Genes Cells* **1**, 59–72.

Schneider, C.A., Rasband, W.S. & Eliceiri, K.W. (2012) NIH Image to ImageJ: 25 years of image analysis. *Nat. Methods* **9**, 671–675.

Shioi, G., Kiyonari, H., Abe, T., Nakao, K., Fujimori, T., Jang, C.W., Huang, C.C., Akiyama, H., Behringer, R.R. & Aizawa, S. (2011) A mouse reporter line to conditionally mark nuclei and cell membranes for in vivo live-imaging. *Genesis* **49**, 570–578.

Soriano, P. (1999) Generalized lacZ expression with the ROSA26 Cre reporter strain. *Nat. Genet.* **21**, 70–71.

Strathdee, D., Ibbotson, H. & Grant, S.G. (2006) Expression of transgenes targeted to the Gt(ROSA)26Sor locus is orientation dependent. *PLoS One* **1**, e4.

Takada, S., Stark, K.L., Shea, M.J., Vassileva, G., McMahon, J.A. & McMahon, A.P. (1994) Wnt-3a regulates somite and tailbud formation in the mouse embryo. *Genes Dev.* **8**, 174–189.

Takemoto, T., Uchikawa, M., Kamachi, Y. & Kondoh, H. (2006) Convergence of Wnt and FGF signals in the genesis of posterior neural plate through activation of the Sox2 enhancer N-1. *Development* **133**, 297–306.

Takemoto, T., Uchikawa, M., Yoshida, M., Bell, D.M., Lovell-Badge, R., Papaioannou, V.E. & Kondoh, H. (2011) Tbx6-dependent Sox2 regulation determines neural or mesodermal fate in axial stem cells. *Nature* **470**, 394–398.

Uchikawa, M., Ishida, Y., Takemoto, T., Kamachi, Y. & Kondoh, H. (2003) Functional analysis of chicken Sox2 enhancers highlights an array of diverse regulatory elements that are conserved in mammals. *Dev. Cell* **4**, 509–519.

Yoshikawa, Y., Fujimori, T., McMahon, A.P. & Takada, S. (1997) Evidence that absence of Wnt-3a signaling promotes neuralization instead of paraxial mesoderm development in the mouse. *Dev. Biol.* **183**, 234–242.

Zambrowicz, B.P., Imamoto, A., Fiering, S., Herzenberg, L.A., Kerr, W.G. & Soriano, P. (1997) Disruption of overlapping transcripts in the ROSA beta geo 26 gene trap strain leads to widespread expression of beta-galactosidase in mouse embryos and hematopoietic cells. *Proc. Natl Acad. Sci. USA* **94**, 3789–3794.

Received: 10 December 2015
Accepted: 29 February 2016

Supporting Information

Additional Supporting Information may be found online in the supporting information tab for this article:

Figure S1 The nucleotide sequence and genetic elements of pWntVis.

Figure S2 Nuclei in the sections shown in Fig. 3C, which were encircled and measured for fluorescence intensities.

Figure S3 Comparison of the response of R26-WntVis and TCF/Lef:H2B-GFP to endogenous Wnt signaling in *Wnt3a*$^{+/+}$ embryos using on-line published data (Ferrer-Vaquer *et al.* 2010).

Table S1 Comparison of various Wnt reporter mouse lines

Table S2 Primer sequences for PCR used for determination of embryo genotypes